Plasma Potential in Toroidal Devices: T-10, TJ-II, CHS and LHD*)

Alexander V. MELNIKOV, Carlos HIDALGO[1)], Takeshi IDO[2)], Akihiro SHIMIZU[2)], Akihide FUJISAWA[3)], Konstantin S. DYABILIN and Sergey E. LYSENKO

Institute of Tokamak Physics, NRC 'Kurchatov Institute', 123182, Moscow, Russia
[1)]*Association EURATOM-CIEMAT, 28040, Madrid, Spain*
[2)]*National Institute for Fusion Science, Toki 509-5292, Japan*
[3)]*Research Institute for Applied Mechanics, Kyushu University, Kasuga 816-8580, Japan*

(Received 9 December 2011 / Accepted 12 June 2012)

Direct measurements of the electric potential φ, using the Heavy Ion Beam Probing, have been undertaken in the T-10 tokamak, and in the helical devices with various magnetic topology: TJ-II, CHS and LHD. L-mode plasmas were considered. Despite the large differences in machine sizes, heating methods and the topology of the magnetic field, the observed φ shows the striking similarities: (i) Similar magnitudes of E_r; (ii) For low densities, $n_e < 0.5 \times 10^{19}$ m^{-3}, φ is positive, and an increase in n_e is associated with the decrease of positive φ and formation of a negative E_r; (iii) For higher densities, $n_e > (0.5\text{-}1) \times 10^{19}$ m^{-3}, both φ and E_r tends to be negative despite the use of different heating methods: Ohmic and ECR heating in T-10, ECRH and/or NBI in TJ-II, CHS and LHD; (iv) Application of ECRH, causing a rise in T_e, results in more positive values for φ and E_r. The analysis show that the main features of the φ dependences on the n_e and T_e agree with neoclassical predictions on the four devices within experimental and simulation precisions.

Keywords: plasma electric potential, radial electric field, HIBP, tokamak, stellarator, neoclassical theory

DOI: 10.1585/pfr.7.2402114

1. Introduction

The direct measurement of the average electric potential in the core plasma is of primary importance for the understanding of the role of the radial electric field E_r in confinement improvement mechanisms [1]. The Heavy Ion Beam Probe (HIBP) is a unique diagnostic to study directly the electric potential and turbulence characteristics in toroidal plasmas from the core to the edge [2, 3]. The HIBP was used in the T-10 circular tokamak [4], in TJ-II, a four-period flexible heliac with helical plasma axis [5] and in the stellarators CHS [6] and LHD [7] to study the potential with high spatial (< 1 cm) and temporal (1 μs) resolution in plasmas with comparable parameters, but in different magnetic configurations. Comparison for Ohmic (OH) and Electron Cyclotron Resonance Heating (ECRH) plasmas in the two machines, T-10 and TJ-II reveals similar tendencies of the potential profiles [8, 9]. The paper reports the results of the comparative studies of plasma potential in all four machines, including CHS and LHD with the same diagnostics. Although the HIBP was used during scans in the main plasma parameters on T-10, TJ-II, CHS and LHD [9–12], and all data obtained in this way were considered in this study. This paper shows only the results obtained on a limited number of interesting discharges in four machines, illustrating our main conclusions. Main engineering parameters for the machines considered are summarized in Table 1.

Table 1 Main parameters of machines under study.

Parameter	T-10	TJ-II	CHS	LHD
$\langle R \rangle$ (m)	1.5	1.5	1.0	3.5 - 4
$\langle a \rangle_{lim}$ (m)	0.3	0.22	0.22	0.63
B_t (T)	1.5 - 2.5	1.0	1.0 - 2.0	0.5 - 2.8
$\bar{n}_e$ (10^{19} m^{-3})	1 - 4	0.2 - 6	0.3 - 3	0.1 - 100
P_{ECRH} (MW)	≤ 2	≤ 0.6	≤ 0.3	≤ 3
P_{NBI} (MW)	–	≤ 0.9	≤ 1.5	≤ 25
E_{HIBP} (keV)	300	125	200	6000
HIBP ions	Tl^+	Cs^+	Cs^+, Rb^+	Au^+
observation area	+0.2<ρ<1	−1<ρ<1	−1 <ρ<1	−1 <ρ<1

2. Electric Potential Profile Evolution in OH, ECR and NBI Heated Plasmas

2.1 Density dependence

Observations with the HIBP diagnostic were undertaken in a large range of OH and ECR heated plasmas in T-10 and in a large range of ECR and NBI heated plasmas in stellarators. Plasma parameters of the discharges studied are shown in Table 1. Ohmic and ECR heated deuterium plasmas with line-averaged density $\overline{n}_e$ = (1.0 - 4.1) × 10^{19} m^{-3} on T-10 are characterized by a negative po-

author's e-mail: melnikov_07@yahoo.com

*) This article is based on the presentation at the 21st International Toki Conference (ITC21).

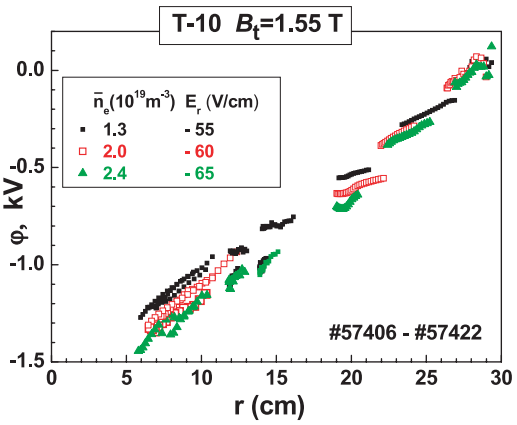

Fig. 1 (a) Ohmic discharge in T-10 with low B_t and rising density $\overline{n}_e$. The radial profiles of plasma potential obtained by a set of radial scans with different E_{HIBP} = (90 - 190) keV for three values of line-averaged central density.

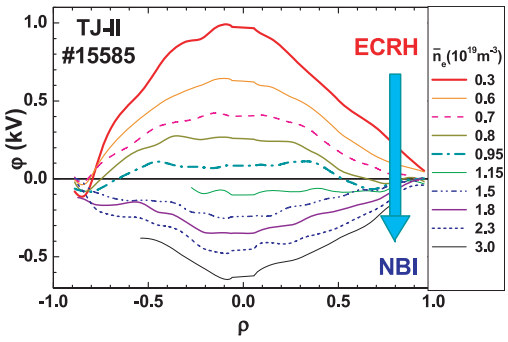

Fig. 2 Evolution of the electric potential profiles with the raise of the line averaged density in plasmas with ECRH and NBI heating on TJ-II. Arrow denotes direction of time evolution.

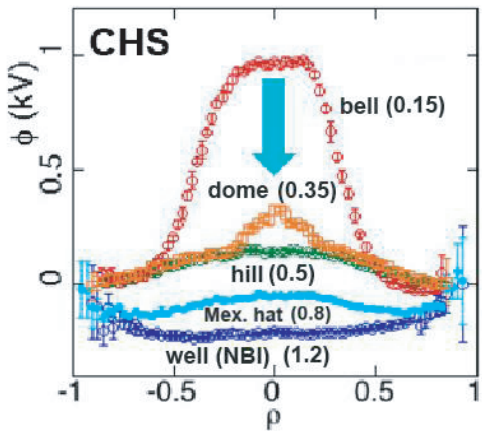

Fig. 3 Evolution of the electric potential profiles with the raise of the line averaged density $\overline{n}_e$ (in brackets, $\times 10^{19}$ m^{-3}) in plasmas with ECRH and NBI heating on CHS.

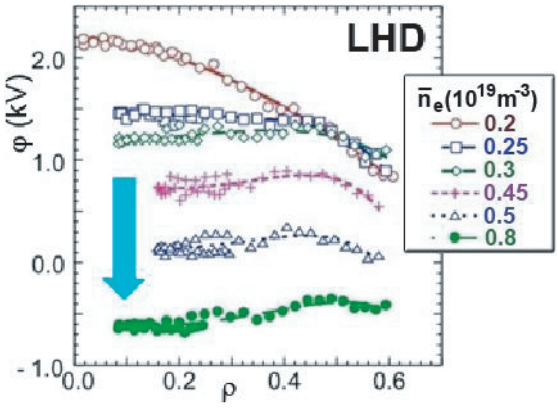

Fig. 4 Evolution of the electric potential profiles with the raise of the line averaged density in plasmas with ECRH and NBI heating on LHD, # 81079.

tential φ up to -1600 V close to plasma centre (ρ = 0.2), where $T_e \sim 1$ keV. As a rule, the potential profile is monotonically increasing towards the plasma edge.

In addition, a density rise due to gas puffing is accompanied by an increasingly more negative potential as presented in Fig. 1.

Plasmas heated with ECR and NBI alone or with combined ECR+NBI heating were studied in TJ-II, CHS and LHD, as presented in Figs. 2, 3, 4. Low-density hydrogen or helium plasmas, $\overline{n}_e < (0.5 - 1) \times 10^{19}$ m^{-3} with ECR heating are characterized by a positive plasma potential in a range up to $\varphi(0) = +2$ kV at the centre of LHD, see Fig. 4. CHS and TJ-II data shows that a small zone with negative plasma potential may appear in the edge depending on the plasma density, see Figs. 2 and 3. The density rise due to gas puff or NBI fuelling is accompanied by a decrease of the plasma potential, which evolves to smaller absolute values, becoming fully negative, if $\overline{n}_e$ exceeds some limit of about 1×10^{19} m^{-3}.

2.2 Electron temperature dependence

On the other hand, a rise in T_e due to an increase in the Ohmic or additional ECR heating (Fig. 2) leads to a decrease in the absolute value of the negative potential in T-10, as shown in Fig. 5. It leads to the increase of the positive potential in TJ-II, CHS and LHD, as presented in Figs. 6, 7 and 8. Generally, the rise in T_e leads to the changes in plasma potential into the positive direction despite the initial value, which was negative in T-10 or positive in CHS, TJ-II and LHD. One should note that the higher density of the target plasmas is associated with lower potential reaction after the ECRH application.

3. Neoclassical Modeling of the Electric Potential Profiles

The neoclassical (NC) modelling was performed for T-10 with Venus +δf code [13], for TJ-II with MOCA code [14], for CHS with Hastings model [6], for LHD with GSRAKE code [15]. The main features of the potential

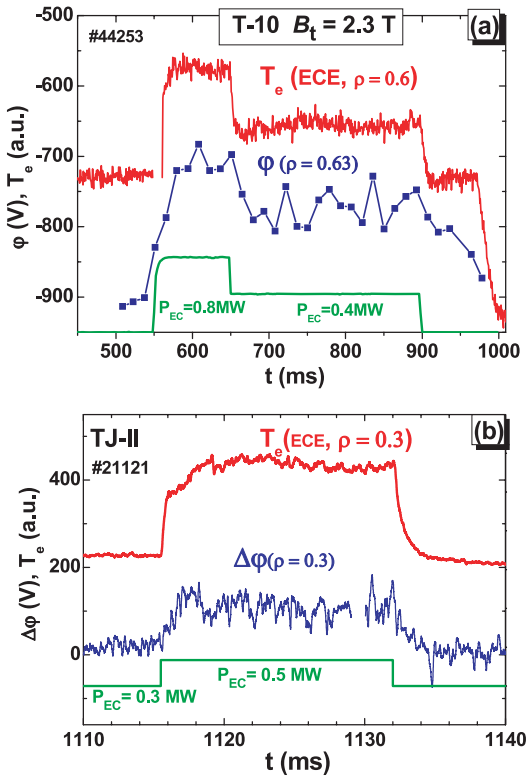

Fig. 5 Time evolution of the plasma potential and T_e in a gradient area at $\rho = 0.63$ for two values of P_{EC} in T-10, B_t = 2.3 T, $\overline{n}_e = 2.2 \times 10^{19}$ m^{-3}, I_p = 185 kA (a) and in the central area at $\rho = 0.3$ in TJ-II, B_t = 1 T, $\overline{n}_e = 0.4 \times 10^{19}$ m^{-3} (b).

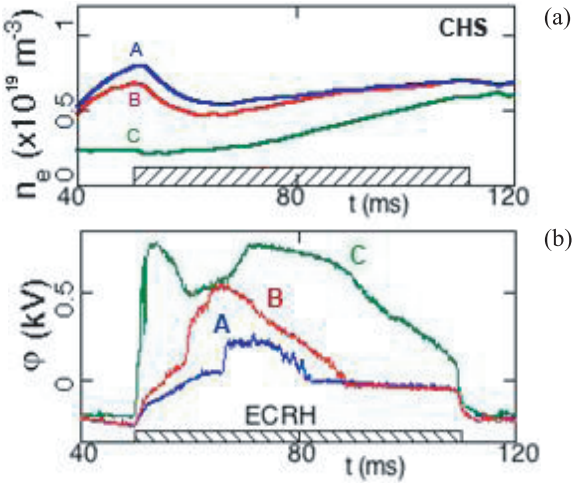

Fig. 6 Time evolution of the plasma potential due to the ECR auxiliary heating in CHS (B_t = 2 T, P_{EC} = 0.2 MW). (a) line-averaged central density for three cases; (b) central plasma potential. The higher density is associated with lower potential.

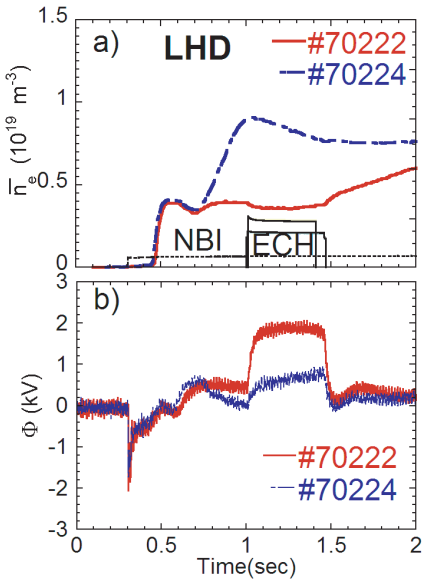

Fig. 7 Time evolution of the potential due to the ECR auxiliary heating in NBI sustained plasma at LHD (B_t = 1.5 T, P_{EC} = 0.88 MW). (a) line-averaged central density; (b) central plasma potential. The higher density is associated with lower potential response to ECRH, similar to the CHS case.

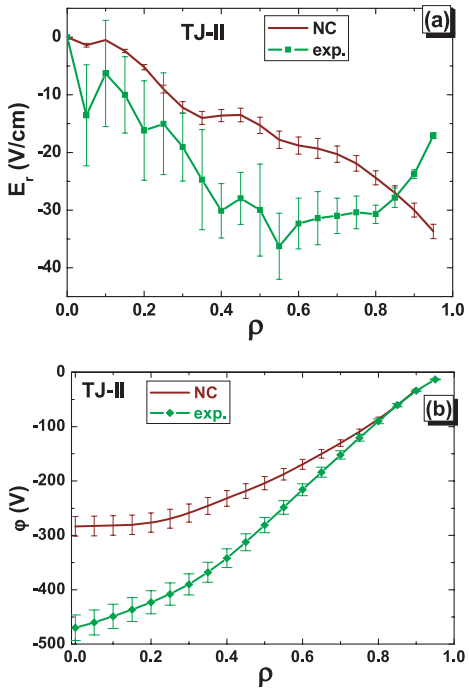

Fig. 8 The radial electric field (a) and potential (b) measured and calculated for the high-density regime with dominated ion losses ($\overline{n}_e = 3 \times 10^{19}$ m^{-3}) in TJ-II.

profiles behavior show quite satisfactory agreement with experimental one [9–11].

Here we show the results of the NC simulations for four machines with simple analytical model [16]. It is based on the tailored long mean free path (lmfp) [17] and plateau [18–20] collisional regimes for the ion and electron fluxes like

$$\Gamma_{i,e} = \Gamma_{i,e}^{lmfp} + \psi_{i,e}\Gamma_{i,e}^{pl}, \quad (1)$$

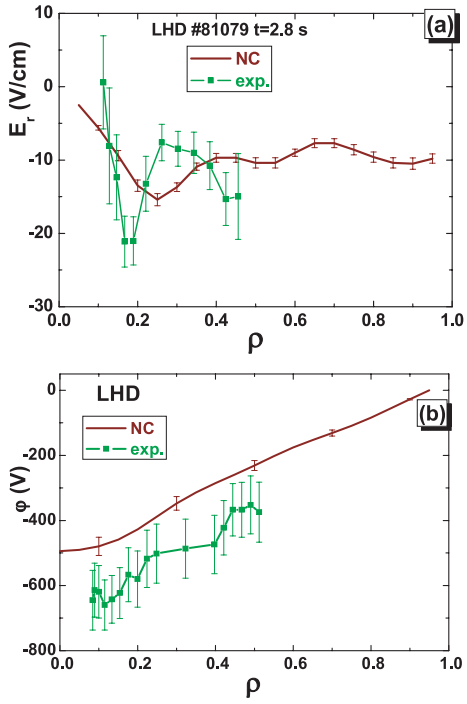

Fig. 9 The radial electric field (a) and potential (b) measured and calculated for the regime with dominated ion losses ($\overline{n}_e = 0.8 \times 10^{19}$ m^{-3}) in LHD.

with the simple smoothing function

$$\psi_{i,e}(\nu_{i,e}/\nu_{i,e}^{eq}) = \nu_{i,e}/(\nu_{i,e} + \nu_{i,e}^{eq}), \quad (2)$$

where

$$\nu_{i,e}^{eq} = \varepsilon_h^{3/2}(v_{i,e} \cdot \hat{\iota}/R), \quad (3)$$

$v_{i,e}$ are thermal velocities, $\hat{\iota}$ is a rotational transform.

To adjust analytical simulations to the complex magnetic structure of stellarators, the effective helical ripple modulation ε_h was adopted from [21] for the particle fluxes in the lmfp case. Thus the ambipolar radial electric field E_r was deduced from the condition

$$\Gamma_e(E_r) = \Gamma_i(E_r). \quad (4)$$

For the high collisional plasmas of the T-10 tokamak, only $\Gamma_{i,e}^{pl}$component remains in the model.

4. Modeling Results

The modeling with the described procedure (1)-(4) was performed for TJ-II and LHD devices for wide range of the collisionality from lmfp to plateau. Figures 8 and 9 show the examples of the E_r and φ modeling compared to experimental data from TJ-II and LHD for the case of the dominant ion losses, which is more relevant to the future fusion devices. Results show that the model qualitatively agrees with experimental φ and E_r profiles.

5. Conclusions

Despite the large differences in machine sizes, heating methods and the topology of the magnetic field, the observed φ shows the striking similarities:
(i) Similar magnitudes of E_r;
(ii) For low densities, $\overline{n}_e < 0.5 \times 10^{19}$ m^{-3} (unattainable in T-10), φ is positive, and an increase in n_e is associated with the decrease of positive φ and formation of a negative E_r;
(iii) For higher densities, $\overline{n}_e > (0.5\text{-}1) \times 10^{19}$ m^{-3}, both φ and E_r tends to be negative despite the use of different heating methods: OH and ECRH in T-10, ECRH and/or NBI in TJ-II, CHS and LHD;
(iv) Application of ECRH, causing a rise in T_e, results in more positive φ and E_r.
(v) The analysis show that for four machines considered the main features of the φ dependences on the n_e and T_e qualitatively agree with neoclassical predictions.

The T-10 team was supported by RFBR grants 10-02-01385 and 11-02-00667, Rosatom H. 4f.45.90.12.1023, and Rosnauka 16.518.11.7004.

[1] G. Van Oost *et al.,* Plasma Phys. Control. Fusion **49,** A29 (2007).
[2] Yu.N. Dnestrovskij *et al.,* IEEE Trans. Plasma Sci. **22**, 310 (1994).
[3] A.J.H. Donné *et al.,* Czech. J. Phys. **55**, 1077 (2002).
[4] A.V. Melnikov *et al.,* Rev. Sci. Instrum. **66**, 317 (1995).
[5] I. Bondarenko *et al.,* Rev. Sci. Instrum. **72**, 583 (2001).
[6] A. Fujisawa *et al.*, Phys. Plasmas **7**, 4152 (2000).
[7] T. Ido *et al.*, Plasma Phys. Control. Fusion **52**, 124025 (2010).
[8] A. Melnikov *et al.*, Fusion Sci. Technol. **31**, 51 (2007).
[9] A. Melnikov *et al.*, Nucl. Fusion **51**, 083043 (2011).
[10] T. Ido *et al.*, Plasma Sci. Technol. **11**, 463 (2009).
[11] A. Fujisawa *et al.*, Plasma Phys. Control. Fusion **44**, A1 (2002).
[12] A. Shimizu *et al.*, Plasma Fusion Res. **2**, S1098 (2007).
[13] M. Isaev *et al.*, EPS-2012, Rep. P2.077.
[14] E. Ascasibar *et al.*, Plasma Phys. Control. Fusion **44**, B307 (2002).
[15] A. Shimizu *et al.*, Plasma Fusion Res. **5**, S1015 (2010).
[16] A. Melnikov *et al.*, Problems of Atomic Sci. Eng. Series Thermonucl. Fusion **3**, 54 (2011) (in Russian).
[17] K.C. Shaing, Phys. Fluids **27**, 1567 (1984).
[18] L.M. Kovrizhnykh, Nucl. Fusion **24**, 851 (1984).
[19] A.A. Galeev and R.Z. Sagdeev, in *Reviews of Plasma Physics*, v. 7, ed. M.A. Leontovich (New York: Consultants Bureau, 1999) p. 257.
[20] T.E. Stringer, Nucl. Fusion **35**, 1008 (1995).
[21] C.D. Beidler *et al.*, Nucl. Fusion **51**, 076001 (2011).